NMR Diffusion and Relaxation Studies of the Encapsulation of Fragrances by Amphiphilic Multiarm Star Block Copolymers

Wolfgang Fieber,[§] Andreas Herrmann,[§] Lahoussine Ouali,[§] Maria Inés Velazco,[§] Georg Kreutzer,[†] Harm-Anton Klok,[†] Céline Ternat,[‡] Christopher J. G. Plummer,[‡] Jan-Anders E. Månson,[‡] and Horst Sommer*[,§]

Firmenich SA, Division Recherche et Développement, B.P. 239, CH-1211 Genève 8, Switzerland, Laboratoire des Polymères (LP), Ecole Polytechnique Fédérale de Lausanne (EPFL), CH-1015 Lausanne, Switzerland, and Laboratoire de Technologie des Composites et Polymères (LTC), Ecole Polytechnique Fédérale de Lausanne (EPFL), CH-1015 Lausanne, Switzerland

Received January 26, 2007; Revised Manuscript Received April 24, 2007

ABSTRACT: Self-diffusion NMR spectroscopy and relaxometry have been employed to study fragrance encapsulation in water-soluble, amphiphilic star block copolymers. Diffusion coefficients of four different fragrance molecules in the free form and in the presence of the polymer have been determined and used to calculate the effective degree of encapsulation. In dilute aqueous solutions between 65% and 99% of the guest molecules are trapped inside the polymer. The degree of encapsulation depends on the hydrophobicity of the guest molecule, expressed by the octanol/water partitioning coefficient (log P_{OW}), where high log P_{OW} molecules are nearly quantitatively dissolved in the polymer. The fragrance molecules are mainly located in the hydrophobic core of the polymer, which is tightly packed, whereas the hydrophilic shell is flexible and takes up only a small percentage. Proton longitudinal (T_1) and transverse (T_2) relaxation times of the fragrance molecules are significantly reduced in the presence of the polymer indicating slower rotational correlation times due to microsolubilization in the hydrophobic core.

Introduction

Delivery systems play a role of increasing importance in fragrance chemistry nowadays.[1−3] Their main task is to guarantee the solubility of less polar, volatile fragrance compounds in typical applications with high water content by entrapping or encapsulating them in a certain type of "amphiphilic" container. These carrier systems are used for the controlled, retarded release of the fragrance molecules as well as for their protection against degradation in order to avoid performance loss. In addition to the classical approach to employ surfactants of different types or surfactant mixtures, synthetic polymers with amphiphilic properties have attracted the attention of researchers in fragrance chemistry during the last years.[4] Tailored polymers as delivery systems are widely known in pharmaceutics where they ensure the transport of active molecules to the intended site of action in order to improve their therapeutic effectiveness.[5−9]

Apart from linear polymers, branched systems like dendrimers[10,11] with different end group functionalities have been developed which are able to interact with various types of organic guest molecules[11−21] and/or exhibit micelle-like properties,[20−23] thus mimicking the behavior of surfactants. Dendrimers have regularly branched, well-defined molecular structures, but are difficult to synthesize. Hyperbranched polymers[5,24,25] are a promising, cheaper alternative, because they can easily be prepared from AB_m type monomers in a one-step synthesis. Disadvantages are imperfect branching and polydispersity, thus making it difficult to characterize them spectroscopically.

* Corresponding author. E-mail: horst.sommer@firmenich.com. Fax: +41 22780 33 34.

[§] Firmenich SA, Division Recherche et Développement.

[†] Laboratoire des Polymères (LP), Ecole Polytechnique Fédérale de Lausanne (EPFL).

[‡] Laboratoire de Technologie des Composites et Polymères (LTC), Ecole Polytechnique Fédérale de Lausanne (EPFL).

We have recently reported the synthesis and characterization of a new class of water-soluble, amphiphilic multiarm star block copolymers.[26,27] The polymers were prepared by sequential atom transfer radical polymerization (ATRP) of *n*-butyl methacrylate (BMA) and poly(ethylene glycol) methyl ether methacrylate (PEGMA), and the resulting compounds with a core−shell architecture were shown to act as host systems for small, hydrophobic fragrance molecules.[26,27] In this connection, it is of importance to gain knowledge about the interaction of these fragrance compounds with their host molecules. Their localization in the host, the amount of molecules entrapped, and effects on the structure of the host due to encapsulation are important questions to address in order to understand and to optimize the properties of the system as a whole.

Self-diffusion NMR spectroscopy and relaxometry are well suited spectroscopic methods in order to answer these questions.[28] Self-diffusion NMR was developed by Stejskal and Tanner in 1965.[29] Since then the technique has proven to deliver detailed insights into the dynamical and structural properties of surfactant systems,[30,31] food model systems,[32] lipid membranes,[33] supramolecular chemicals,[34] proteins,[35] and polymers.[36,37] Some dendrimeric systems have also been investigated.[38−40] The dependence of the diffusion coefficients on generation number, concentration and temperature revealed information about the structure and the size of the dendrimers as well as aggregation effects in solution.

To study this new class of water-soluble, amphiphilic multiarm star block copolymers in more detail we employed self-diffusion NMR to determine the diffusion coefficients of the polymeric hosts and the fragrance molecules in D_2O solutions, which yielded information about the solubilization and partitioning of fragrance compounds in these systems. Longitudinal and transversal relaxation times (T_1, T_2) were measured to support the findings and to achieve information

10.1021/ma070222i CCC: $37.00
Published on Web 06/28/2007

Chart 1. Structures of the Fragrance Molecules Used for the Encapsulation Studies

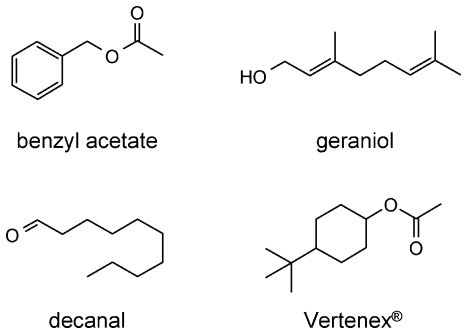

Chart 2. Average Structure of the Boltorn HBP H40 Functional Core

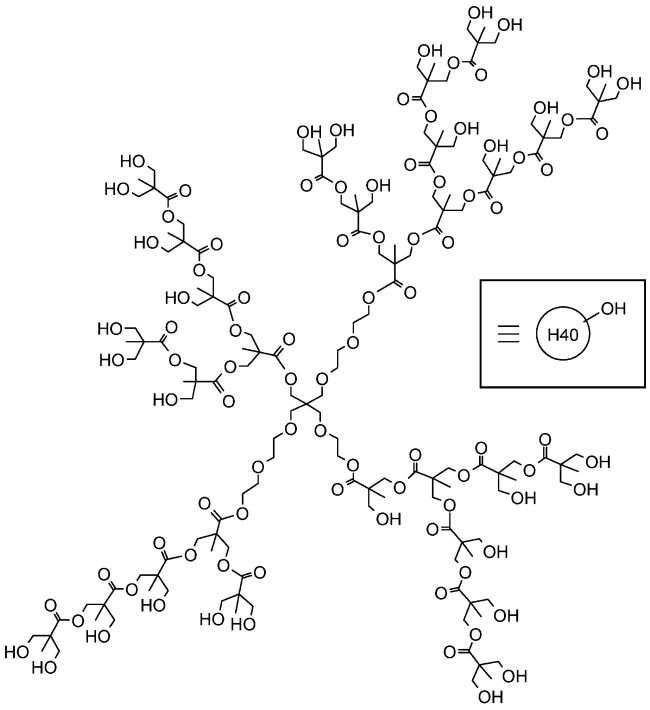

about the localization of the fragrance molecules and the internal dynamics of the host−guest system.

Experimental Section

Materials. Benzyl acetate, geraniol (trans-3,7-dimethyl-2,6-octadien-1-ol), decanal, and Vertenex (4-*tert*-butylcyclohexyl acetate, Chart 1) are commercially available perfumery commodities which were used without further purification. The log P_{OW} values (octanol/water partitioning coefficients)[41,42] of the fragrance molecules were determined by HPLC (benzyl acetate, 2.04; geraniol, 2.97; decanal, 4.00; Vertenex, 4.47). Polymers investigated in this study were based on a commercially available fourth generation hyperbranched polyester core (Boltorn H40, Chart 2) which was either functionalized with a hydrophobic poly(*n*-butyl methacrylate) (PBMA) inner shell and a hydrophilic poly[poly(ethylene glycol) methyl ether methacrylate] (PPEGMA) outer shell to give H40-$PBMA_{37}$-*b*-$PPEGMA_{39}$ or only with a hydrophilic PPEGMA shell to give H40-$PPEGMA_{50}$ (Chart 3). These samples, both having roughly the same total average molecular weights, were synthesized as reported previously.[26]

Sample Preparation. Solutions of 1 wt % H40-$PBMA_{37}$-*b*-$PPEGMA_{39}$ and 1.2 wt % H40-$PPEGMA_{50}$ in D_2O were prepared. An excess amount of fragrance oil was added and the sample was sealed and shaken at room temperature overnight. Samples of the free form of the fragrance molecules were prepared by dissolving 1 μL of the fragrance oil in 700 μL D_2O. For high log P_{OW} samples, further dilution was necessary in order to obtain the monomeric form.

Chart 3. Schematic Representation of Polymers H40-$PBMA_{37}$-*b*-$PPEGMA_{39}$ and H40-$PPEGMA_{50}$

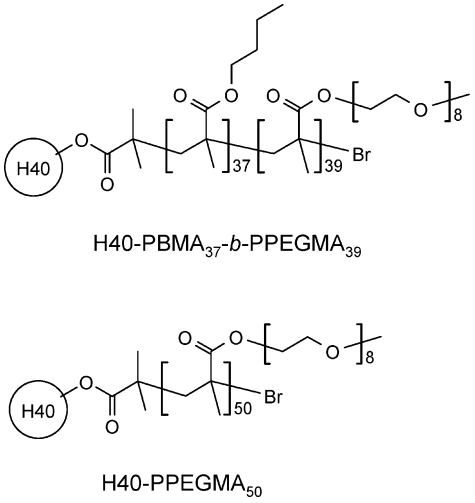

NMR Spectroscopy. NMR diffusion measurements were recorded at 25 °C on a Bruker 400 MHz Avance II system equipped with a 5 mm diffusion probe (Bruker Diff 30). The gradient amplitude was calibrated to 1215 G cm^{-1} at maximum intensity by means of a sample of doped water and diffusion coefficients from literature. Diffusion coefficients were obtained from a stimulated echo pulse sequence.[43] In a typical experiment, 16 spectra were recorded with increasing gradient strength, where gradient pulse duration (1−2 ms), diffusion delay (20−40 ms), and maximal gradient strength were adjusted for each molecule in the mixture in order to obtain a complete decay of the diffusion curve. The amplitudes in the diffusion decay are expressed as the ratio of the observed signal intensities in the experiment and the signal intensity that would be observed at zero gradient strength:[43−45]

$$I/I_0 = \exp[-\gamma^2\,\delta^2\,g^2\,(\Delta-\delta/3)\,D] \qquad \text{(eq 1)}$$

where γ is the gyromagnetic ratio, δ is the gradient pulse duration, g is the gradient amplitude, Δ is the diffusion delay in the NMR experiment, and D is the diffusion coefficient. All experiments were analyzed using Bruker TopSpin 1.3 or XWIN-NMR 3.2 software. Diffusion decays were fit to monoexponential decay functions. The signal of the poly(ethylene glycol) moiety was used for the determination of the diffusion coefficient of the polymer, whereas for the fragrance molecules each signal that did not overlap with the polymer resonances was analyzed separately. The deviation of the obtained diffusion coefficients was usually less than 5%. The program CONTIN[46,47] that uses the inverse Laplace transformation for the determination of distributions of decay rates was used for the analysis of the polydispersity of H40-$PBMA_{37}$-*b*-$PPEGMA_{39}$.

On the basis of a two-site model the effective degree of encapsulation of fragrance molecules in the polymer was determined by

$$f_{enc} = (D_{frag}{}^{free} - D_{frag}{}^{enc})/(D_{frag}{}^{free} - D_{poly}{}^{enc}) \qquad \text{(eq 2)}$$

where $D_{frag}{}^{free}$ and $D_{frag}{}^{enc}$ are the diffusion coefficients of the fragrance molecule in the free and the encapsulated forms, and $D_{poly}{}^{enc}$ is the diffusion coefficient of the polymer in the presence of the fragrance molecule.

Relaxation experiments were carried out on Bruker 400 MHz Avance II or Bruker 500 MHz Avance instruments. Longitudinal T_1 and transverse T_2 relaxation times were obtained from inversion−recovery and CPMG experiments, respectively, with a relaxation delay between single scans that was in all cases larger than or

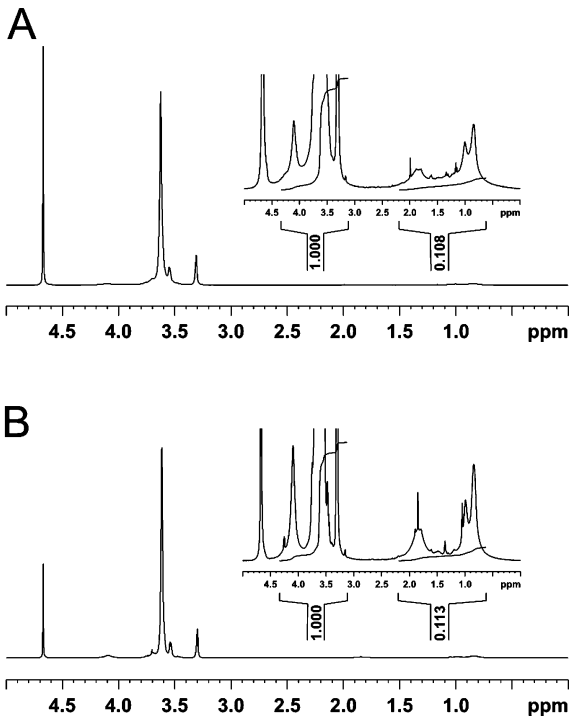

Figure 1. ^{1}H NMR spectra of H40-PBMA$_{37}$-*b*-PPEGMA$_{39}$ (A) and H40-PPEGMA$_{50}$ (B) in D_2O at 25 °C. The peaks at 4.67 ppm are due to residual H_2O in the solvent. The same spectra but with the ordinate enlarged in order to see the peaks in the aliphatic regions are depicted in the insets.

equal to 5 × T_1. Relaxation times were measured for individual methyl groups in the fragrance molecules (benzyl acetate, CH_3−CO, δ = 2.02 ppm; geraniol, CH_3−C(CH$_3$)=C, δ = 1.52 ppm; decanal, CH_3−CH$_2$, δ = 0.75 ppm; Vertenex, (CH_3)$_3$−C, δ = 0.74 ppm). A monoexponential fitting was applied to all relaxation curves.

For the titration series of H40-PBMA$_{37}$-*b*-PPEGMA$_{39}$ with benzyl acetate several solutions of the polymer were prepared to which exact quantities of the fragrance oil were added. DMSO was used as an internal standard. Experiments were carried out with a relaxation delay of 25 s and acquisition time of 5 s, and integrals were measured for the DMSO peak and the aromatic signals of benzyl acetate, respectively.

Results and Discussion

Polymer Structure and Dynamics. The ^{1}H NMR spectrum of H40-PBMA$_{37}$-*b*-PPEGMA$_{39}$ in D_2O is dominated by the peaks corresponding to the protons of the poly(ethylene glycol) moiety of the PPEGMA hydrophilic shell (Figure 1). Chemical shifts can be resolved for the terminal methyl group (3.31 ppm) and the first (4.11 ppm) and the last methylene groups (3.55 ppm) in the PEG side chain, respectively, whereas all other methylene groups overlap (3.63 ppm). In the aliphatic region very broad signals corresponding to the protons of the backbone of the PEGMA building blocks are found (2.1−0.7 ppm). Compared to the spectrum in D_2O of H40-PPEGMA$_{50}$, a polymer that lacks the hydrophobic core and where the NMR signals necessarily correspond to the PEGMA units only, no additional peaks can be detected, and the ratios of the integrals of the PPEGMA side chain and backbone protons are the same for both molecules (Figure 1). Hence, protons in the hydrophobic PBMA core of the polymer are invisible in the NMR spectrum of H40-PBMA$_{37}$-*b*-PPEGMA$_{39}$.

Longitudinal T_1 and transverse T_2 proton relaxation times were used to identify the dynamic properties in the hydrophilic shell of H40-PBMA$_{37}$-*b*-PPEGMA$_{39}$. A sharp decrease of both

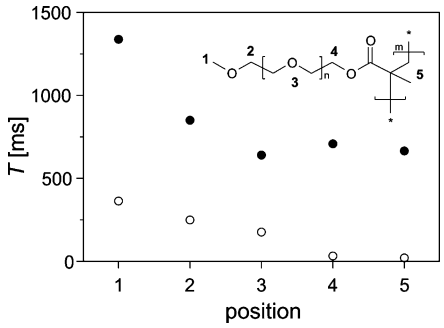

Figure 2. Longitudinal T_1 (full circles) and transverse T_2 (open circles) proton relaxation times at 500 MHz as a function of the position in the PEGMA unit of H40-PBMA$_{37}$-*b*-PPEGMA$_{39}$.

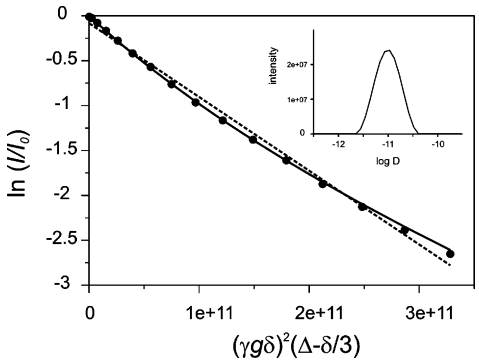

Figure 3. Semilogarithmic plot of the attenuation of the NMR signal at 3.63 ppm in the STE diffusion experiment of H40-PBMA$_{37}$-*b*-PPEGMA$_{39}$ as a function of the gradient strength *g*. The dotted and the full lines represent fitting curves due to linear regression and CONTIN analysis, respectively. The inset depicts the distribution of diffusion coefficients that was obtained from the CONTIN analysis.

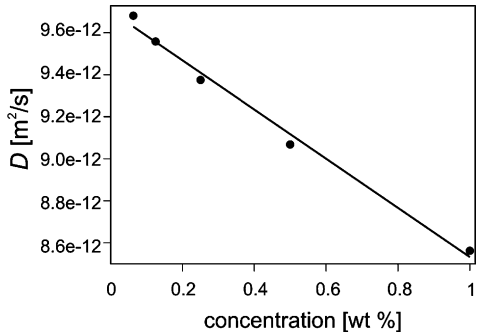

Figure 4. Diffusion coefficients of H40-PBMA$_{37}$-*b*-PPEGMA$_{39}$ at various concentrations of the polymer. Data were fit by linear regression.

T_1 and T_2 times can be observed starting from the terminal methyl groups toward the central methylene groups of the PEG side chains indicating that the mobility is highest at the end of the chain and decreases when the backbone is approached (Figure 2). T_2 times continue to decrease from the innermost methylene group to the aliphatic protons of the backbone. Apparently, dynamics are more restricted in these parts. Since reorientation about chemical bonds in this part of the molecule requires the concerted motion of large groups attached to them, dynamics are highly decreased leading to long rotational correlation times and low T_2 values. In contrast, T_1 times in these regions do not decrease further but are even slightly higher. Compared to the highly mobile, terminal protons that lie in the extreme narrowing region, backbone protons presumably lie on the right side of the T_1 minimum, where T_1 times increase and T_2 times decrease as a function of the rotational correlation time.[38] It has to be mentioned that transverse T_2 relaxation decays of H40-PBMA$_{37}$-*b*-PPEGMA$_{39}$ have been fit to

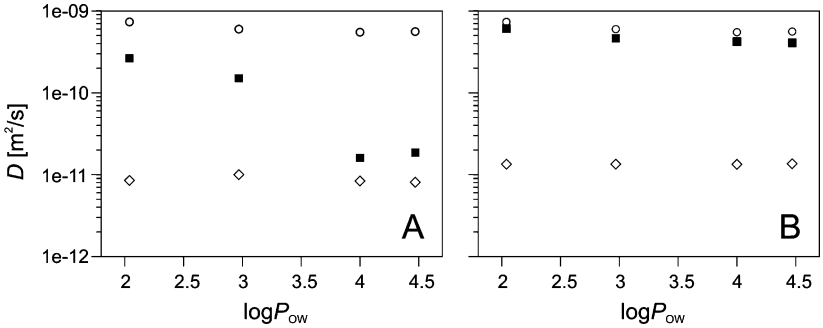

Figure 5. Encapsulation of different fragrance molecules in solutions of H40-PBMA$_{37}$-*b*-PPEGMA$_{39}$ (A) and H40-PPEGMA$_{50}$ (B). Fragrance molecules were benzyl acetate (log P_{OW} 2.04), geraniol (2.97), decanal (4.00), and Vertenex (4.47). Diffusion coefficients are depicted for the fragrance molecules in the free form (open circles) and encapsulated form (filled squares), respectively, and for the polymer (open diamonds).

Table 1. Proton Relaxation Data at 500 MHz of Fragrance Molecules in the Free Form and Encapsulated Form in H40-PBMA$_{37}$-*b*-PPEGMA$_{39}$

	log P_{OW}	T_1^{free} [ms][a]	T_1^{enc} [ms]	T_2^{free} [ms]	T_2^{enc} [ms]	T_1/T_2^{free}	T_1/T_2^{enc}
benzyl acetate	2.04	4098 ± 17	2118 ± 7	3751 ± 13	566 ± 2	1.09	3.74
geraniol	2.97	3103 ± 20	1282 ± 18	1627 ± 23	158 ± 2	1.91	8.11
decanal	4.00	2475 ± 27	944 ± 6	776 ± 47	123 ± 8	3.19	7.67
Vertenex	4.47	944 ± 4	588 ± 10	928 ± 10	15 ± 1	1.02	39.2

[a] T_1 and T_2 times were determined at specific methyl positions in the individual molecules. For details see Materials and Methods.

monoexponential fitting functions, while they rather show a superposition of more than one exponential function. This is not surprising for such a system, and it reflects local differences in dynamics in the hydrophilic shell as these locations are not shift-resolvable. Moreover, it has been demonstrated by gel permeation chromatography (GPC) that the molecular weight distribution of H40-PBMA$_{37}$-*b*-PPEGMA$_{39}$ is polydisperse ($M_w/M_n = 2.04$)[26] and differences in T_2 values could arise between the individual components of the mixture.

These data show the large range of amplitudes that govern internal mobility in H40-PBMA$_{37}$-*b*-PPEGMA$_{39}$. The outer PPEGMA layer of the polymer is flexible, and relaxation measurements indicate good solubilization and the absence of strong interactions between the individual arms. On the other hand, resonance lines in the hydrophobic PBMA section are broadened beyond detection limit due to highly restricted, solid-state like dynamics. Here, transverse relaxation is dominated by the overall tumbling of the molecule that is very slow according to its high molecular weight of 782 kDa.[26] In contrast, when H40-PBMA$_{37}$-*b*-PPEGMA$_{39}$ was dissolved in the much less polar solvent $CDCl_3$ PBMA signals could well be detected (data not shown). Thus, the complete cancellation of PBMA signals in D_2O seems to reflect the tight packing of backbone and sidechains in order to exclude the polar water molecules. These findings confirm the microphase separated structure of a spherical core and a diffuse PPEGMA corona determined by differential scanning calorimetry (DSC) and small-angle X-ray scattering (SAXS) measurements.[26]

Self-Diffusion of H40-PBMA$_{37}$-*b*-PPEGMA$_{39}$. The simulated echo pulse sequence[43] was used to determine the diffusion coefficients of H40-PBMA$_{37}$-*b*-PPEGMA$_{39}$. Monoexponential curve fitting yields a diffusion coefficient of 8.50×10^{-12} m^2/s. From a semilogarithmic plot, however, it is obvious that the measured values do not decay in a straight line as it would be expected for the isotropic diffusion of a monodisperse molecule (Figure 3). This behavior is rather due to the polydisperse nature of H40-PBMA$_{37}$-*b*-PPEGMA$_{39}$. The program CONTIN is especially designed for the analysis of such samples,[46,47] where continuous distributions of diffusion coefficients are determined by means of the inverse Laplace transformation.[48,49] The result of the CONTIN fit of the diffusion experiment of H40-PBMA$_{37}$-*b*-PPEGMA$_{39}$ shows an excellent correlation with the experimental data (Figure 3). A Gaussian distribution of diffusion coefficients is obtained that is centered at 9.3×10^{-12} m^2/s and has a full width at half-maximum of 1.57×10^{-11} m^2/s (see inset, Figure 3).

A concentration series was carried out in order to calculate the effective hydrodynamic radius from the Stokes−Einstein equation at infinite dilution D_0.[39,50] Extrapolation from linear regression of the diffusion coefficients that were measured between 1 and 0.06 wt % yields a D_0 of 9.70×10^{-12} m^2/s (Figure 4). Using this value and the viscosity of D_2O at 25 °C[51] in the equation, a hydrodynamic radius R_H of 20.5 nm is obtained. We reported previously a radius of gyration R_G of 12.2 nm that was determined from SAXS measurement[26] and fit to the model of Pedersen and Gerstenberg.[52,53] Taking into account the known relationship between R_H and R_G for spherical molecules, $R_G = 0.775R_H$,[54,55] both values are in good agreement.

Fragrance Encapsulation. We demonstrated already by NMR spectroscopy that fragrance molecules are effectively encapsulated in the amphiphilic copolymers.[26] Here we extend the analysis to self-diffusion NMR and relaxometry. Both techniques report on molecular motion, but the type and time scales are different. Whereas relaxometry reports on rotation and internal motions in the pico- to nanosecond time regime, diffusion NMR probes translation in the millisecond to second time regime.

The determination of diffusion data for each individual compound in a mixture is the outstanding advantage of self-diffusion NMR. According to Stokes' law diffusion coefficients of fragrance and polymer molecules are distinct from each other due to their large difference in molecular weight. When a fragrance molecule enters the polymer, however, it will travel with the speed of the host molecule. Since the exchange between the free and the encapsulated forms is an equilibrium process the measured diffusion coefficient is a weighted, average value. Thus, the effective degree of encapsulation can be calculated when the diffusion coefficients of fragrance molecules in the free form and in the presence of the polymer are determined.

Four fragrance molecules were chosen that span a large range of log P_{OW} values (2−4.5). As it can be seen in Figure 5A the diffusion coefficients of all fragrance molecules in the presence

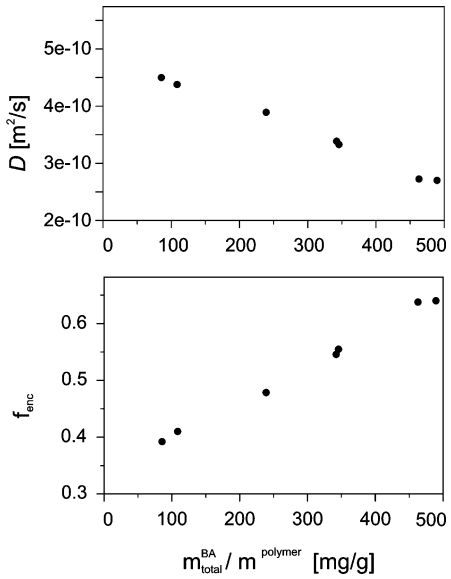

Figure 6. (A) Diffusion coefficients of benzyl acetate at different concentrations in 1 wt % solutions of H40-PBMA$_{37}$-*b*-PPEGMA$_{39}$, where the sample at highest concentration represents the saturated form. The amount of benzyl acetate was calculated from DMSO as internal standard and is the total of free and encapsulated molecules in each sample. (B) Degree of encapsulation of benzyl acetate in 1 wt % solutions of H40-PBMA$_{37}$-*b*-PPEGMA$_{39}$ as a function of total concentration of benzyl acetate in the polymer solution.

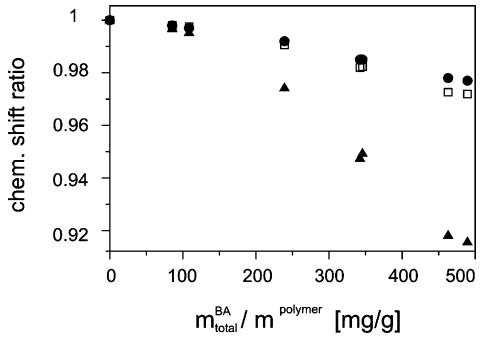

Figure 7. Proton chemical shifts of benzyl acetate in 1 wt % solutions of H40-PBMA$_{37}$-*b*-PPEGMA$_{39}$ normalized on the shifts of the free form (arbitrarily set to the origin of the abscissa). The values for aromatic protons (filled circles), methylene protons (open squares), and methyl protons (filled triangles) are depicted as a function of the total concentration of benzyl acetate in the polymer solution.

of H40-PBMA$_{37}$-*b*-PPEGMA$_{39}$ are significantly lower than that of the free forms proving successful encapsulation. The absolute values, however, depend on the type of molecule under investigation. Using the log P_{OW} value as the parameter of comparison, the diffusion coefficients of the encapsulated fragrance molecules approach the values of the polymer as a function of log P_{OW}. The relative amount that is encapsulated in H40-PBMA$_{37}$-*b*-PPEGMA$_{39}$ increases from 65% for benzyl acetate, 76% for geraniol, to 99% for decanal and 98% for Vertenex, respectively, showing a nearly complete uptake of high log P_{OW} molecules. Generally, diffusion decay curves of the fragrance molecules are not bi- but monoexponential indicating fast exchange between the free and encapsulated forms,[56] but for high log P_{OW} molecules we observe a similar diffusion decay as for the polymer itself due to polydispersity. The observed relationship between the degree of encapsulation and the log P_{OW} value appears reasonable, as high log P_{OW} molecules have a low solubility in water and are likely to prefer the environment in the hydrophobic core of the polymer rather than low log P_{OW} molecules that are much better water-soluble. The size of the polymer is not correlated with the amount of encapsulated guest molecules. It increases to some extent for benzyl acetate (2.5% decrease of diffusion coefficient), decanal (3.4%), and Vertenex (6.1%). However, the reversed effect has been observed for geraniol where the size of the polymer decreases (18% increase of diffusion coefficient). The effective size seems rather to be influenced by structural changes of the polymer as a function of the nature of the encapsulated molecule. Fragrance molecules are mainly located in the hydrophobic core of the polymer. In the presence of H40-PPEGMA$_{50}$, which contains the PPEGMA shell but lacks the hydrophobic core, the diffusion coefficients of the fragrance molecules decrease only little compared to the free forms (Figure 5B). The degree of encapsulation is only between 17% (benzyl acetate) and 28% (Vertenex). Similar results were obtained from quantitative NMR studies.[26]

Proton relaxation data of fragrance molecules are good indicators for encapsulation, too. Longitudinal (T_1) and transverse (T_2) relaxation times of the four fragrance compounds decreased dramatically in the presence of H40-PBMA$_{37}$-*b*-PPEGMA$_{39}$ (Table 1). This is compatible with a restriction of the dynamics of the small molecules due to encapsulation.[57] Relaxation data can be used to estimate the overall rotational correlation time τ_c when expressed as the ratio T_1/T_2.[58] The values of the encapsulated forms are significantly higher than that of the free forms, showing a substantial slowing down of the rotational tumbling upon encapsulation in the polymer. Additionally, T_1/T_2 ratios are very much depended on the nature of the molecule itself, and for high log P_{OW} molecules we find values that are ten times larger than for low log P_{OW} molecules. This may be a consequence of the increasing degree of encapsulation as a function of log P_{OW} that has been observed with diffusion NMR, as the apparent rotational correlation time reflects a weighted average over free and encapsulated forms. However, relaxation data inherently depend on the direct chemical environment of the protons, which hampers a quantitative comparison of different molecules. In addition to that, binding affinities and interactions inside the polymer may be different for each fragrance molecule, and due to the equilibrium nature of the exchange process, relaxation values for the pure bound states are not accessible.

It is interesting to note that although dynamics in the inner core are highly restricted and protons of the polymer are invisible to NMR detection, fragrance molecules that are dissolved therein still give rise to NMR signals in a quantitative manner. However, relaxation data prove the presence of slow motion once the guest molecules are encapsulated in the polymer. It seems thus that they are mainly microsolubilized in the hydrophobic core of the polymer rather than forming oil droplets, but the encapsulated molecules still possess enough degrees of freedom of rotation and fast exchange with the free form in bulk solution.

Titration of H40-PBMA$_{37}$-*b*-PPEGMA$_{39}$ with Benzyl Acetate. In the previous experiments, we measured fragrance encapsulation in saturated solutions. In order to obtain information about the actual chemical equilibrium of polymer and fragrance molecules a titration series was carried out where increasing amounts of benzyl acetate were added to the polymer solution until finally saturation was achieved. Benzyl acetate was chosen for two reasons. First, it is encapsulated in higher amounts than the other fragrance molecules studied, which facilitates the addition of minute amounts in the sample preparation. Second, the fraction of the free form is still

Table 2. Proton Relaxation Data at 400 MHz of Benzyl Acetate Encapsulated in H40-PBMA$_{37}$-*b*-PPEGMA$_{39}$

mass ratio [mg/g][a]	T_1 (H^{arom}) [ms]	T_2 (H^{arom}) [ms]	T_1/T_2 (H^{arom})	T_1 (CH_2) [ms]	T_2 (CH_2) [ms]	T_1/T_2 (CH_2)	T_1 (CH_3) [ms]	T_2 (CH_3) [ms]	T_1/T_2 (CH_3)
0[b]	7111 ± 20	5215 ± 28	1.36	3180 ± 7	2592 ± 29	1.23	4482 ± 20	3832 ± 17	1.17
85.5[c]	845 ± 20	36 ± 1	23.3	n.d.	n.d.	n.d.	829 ± 17	40 ± 1	20.8
109	842 ± 22	59 ± 1	14.3	768 ± 12	n.d.	n.d.	872 ± 13	70 ± 2	12.4
239	1455 ± 33	340 ± 2	4.28	1053 ± 13	213 ± 4	4.94	1320 ± 12	373 ± 5	3.54
342[c]	1927 ± 23	462 ± 8	4.17	1271 ± 12	322 ± 5	3.95	1686 ± 13	461 ± 6	3.66
346	1720 ± 15	493 ± 6	3.49	1132 ± 7	399 ± 9	2.83	1463 ± 9	551 ± 4	2.66
463	1895 ± 5	521 ± 5	3.64	1206 ± 5	449 ± 5	2.69	1467 ± 12	520 ± 5	2.82
489	1988 ± 6	595 ± 4	3.34	1252 ± 7	495 ± 5	2.53	1632 ± 7	532 ± 6	3.07

[a] Total mass of benzyl acetate in solution per mass of H40-PBMA$_{37}$-*b*-PPEGMA$_{39}$. [b] Solution of 1% benzyl acetate in D_2O without polymer. [c] Data determined at 500 MHz.

significant and the system can be studied under equilibrium conditions between free and encapsulated forms.

By increasing the amount of benzyl acetate that is added to a 1 wt % solution of H40-PBMA$_{37}$-*b*-PPEGMA$_{39}$ the diffusion coefficient of the fragrance molecule decreases (Figure 6). According to eq 2, the degree of encapsulation increases continuously with the amount of benzyl acetate added. It seems that the encapsulation process is an equilibrium process between the two phases, i.e., water phase and the hydrophobic particle interior, respectively, where the equilibrium is shifted to the right side by increasing the amount of the fragrance molecules. The mole fraction in the polymer increases from 40% at a total amount of benzyl acetate in solution of 86 mg/g of polymer to 64% in the saturated form (489 mg benzyl acetate/g of polymer). The maximum load of benzyl acetate in the polymer is thus 313 mg/g of polymer. This amount seems to be related to the extent of the hydrophobic core. In H40-PBMA$_{58}$-*b*-PPEGMA$_{40}$,[26] a polymer where the PBMA element is approximately 60% longer, the maximum load is more than doubled (700 mg benzyl acetate/g of polymer, data not shown).

In Figure 7, the chemical shifts of benzyl acetate normalized to that of the free form are depicted for all protons. They are continuously shifted toward the high field upon the addition of benzyl acetate to the polymer solution. Whereas the changes for aromatic and methylene protons are moderate, methyl protons experience a significant high field shift from 2.05 ppm in the free form to 1.88 ppm in the saturated form.

The picture is different when looking at proton T_1 and T_2 relaxation times of the fragrance molecules (Table 2). There is a sudden decrease from the free form of benzyl acetate to the situation when H40-PBMA$_{37}$-*b*-PPEGMA$_{39}$ is present, and T_1 and T_2 times drop from several seconds to around 800 and 50 ms, respectively. However, with the further addition of benzyl acetate the effect is reversed and both T_1 and T_2 times increase continuously toward the saturated state. This can be clearly illustrated by comparing the T_1/T_2 ratios as a function of fragrance concentrations. The values are highest at low concentration of benzyl acetate and decrease continuously toward the value of the saturated form, indicating a higher percentage of slow motion when only very little perfume oil is present.

The hydrophobic core of the polymer may represent a heterogeneous container for fragrance molecules with binding sites that differ in accessibility and mobility. In the presence of small amounts of benzyl acetate, the relaxation values indicate slow motion and restricted dynamics consistent with the positioning of the molecule in a rather rigid environment, probably the very inner part of the polymer, where the space between the individual arms is small. Fragrance molecules that are added subsequently may be located elsewhere in the hydrophobic core where the conformational restriction is less strong, leading to an increase in T_1 and T_2 relaxation times. On the other hand, the observed effects may also be attributed to plasticizing effects of benzyl acetate in that it would render the polymer chains in the hydrophobic core more mobile and with it the microsolubilized fragrance molecules. In fact, in the NMR spectrum of H40-PBMA$_{37}$-*b*-PPEGMA$_{39}$ in D_2O in the presence of benzyl acetate additional broad peaks appear in the aliphatic region (data not shown) that presumably correspond to the PBMA units of the polymer core that are otherwise not detectable.

Conclusions

In the present work, we have shown the encapsulation of hydrophobic guest molecules in hyperbranched star block copolymers by diffusion NMR and proton relaxation measurements. The data show the successful concept of the new class of core−shell polymer delivery systems.[59] Hydrophobic guest molecules are mainly dissolved in the hydrophobic core. The degree of encapsulation is strongly log P_{OW} dependent, and high log P_{OW} molecules are nearly quantitatively dissolved in the polymer. The core−shell architecture can be described by a microphase separated structure. The hydrophobic core is rigid and the protons are not detectable in the NMR spectrum in D_2O. On the other hand, the hydrophilic PPEGMA part is highly mobile, where the mobility decreases from the terminal groups of the side chain toward the backbone. Encapsulation of fragrance molecules is an equilibrium process and the exchange between free and encapsulated forms is fast on the NMR time scale.

Acknowledgment. The Swiss CTI Technology Oriented Program (TOP) Nano 21 is acknowledged for its financial support. We thank Dr. Christine Vuilleumier (Firmenich SA) for the measurement of log P_{OW} values of the fragrance molecules.

References and Notes

(1) Gautschi, M.; Bajgrowicz, J. A.; Kraft, P. *Chimia* **2001**, *55*, 379−387.
(2) Park, S.-J.; Arshady, R. *Microspheres, Microcapsules Liposomes* **2003**, *6*, 157−198.
(3) Ness, J.; Simonsen, O.; Symes, K. *Microspheres, Microcapsules Liposomes* **2003**, *6*, 199−234.
(4) Berthier, D.; Ouali, L. PCT Int. Patent Appl., WO 2005/108471, 2005.
(5) Uhrich, K. E. *Trends Polym. Sci.* **1997**, *5*, 388−393.
(6) Uhrich, K. E.; Cannizzaro, S. M.; Langer, R. S.; Shakesheff, K. M. *Chem. Rev.* **1999**, 3181−3198.
(7) Duncan, R. *Nat. Rev. Drug. Disc.* **2003**, *2*, 347−360.
(8) Hoste, K.; De Winne, K.; Schacht, E. *Int. J. Pharm.* **2004**, *277*, 119−131.
(9) D'Souza, J. M.; Topp, E. M. *J. Pharm. Sci.* **2004**, *93*, 1962−1979.
(10) Newkome, G. R.; Moorefield, C. N.; Vögtle, F. *Dendrimers and Dendrons−Concepts, Syntheses, Applications*; Wiley-VCH, Weinheim, Germany, 2001.
(11) *Dendrimers and Other Dendritic Polymers*; Fréchet, J. M. J., Tomalia, D. A., Eds.; Wiley Series in Polymer Science; Wiley: Chichester, U.K., 2001.
(12) Baars, M. W. P. L.; Meijer, E. W. *Top. Curr. Chem.* **2000**, *210*, 131−182.

(13) Smith, D. K.; Diederich, F. *Top. Curr. Chem.* **2000**, *210*, 183−227.
(14) Liu, M.; Kono, K.; Fréchet, J. M. J. *J. Controlled Release* **2000**, *65*, 121−131.
(15) Zimmerman, S. C.; Lawless, L. J. *Top. Curr. Chem.* **2001**, *217*, 95−120.
(16) Hecht, S.; Fréchet, J. M. J. *Angew. Chem., Int. Ed.* **2001**, *40*, 74−91.
(17) Stiriba, S.-E.; Frey, H.; Haag, R. *Angew. Chem., Int. Ed.* **2002**, *41*, 1329−1334.
(18) Svenson, S.; Tomalia, D. A. *Adv. Drug Delivery Rev.* **2005**, *57*, 2106−2129.
(19) D'Emanuele, A.; Attwood, D. *Adv. Drug Delivery Rev.* **2005**, *57*, 2147−2162.
(20) Bosman, A. W.; Janssen, H. M.; Meijer, E. W. *Chem. Rev.* **1999**, *99*, 1665−1688.
(21) Moorefield, C. N.; Newkome, G. R. *C. R. Chimie* **2003**, *6*, 715−724.
(22) van Genderen, M. H. P.; de Brabander-Van, Den, Berg, E. M. M.; Meijer, E. W. *Adv. Dendritic Macromol.* **1999**, *4*, 61−105.
(23) Dufresne, M.-H.; Fournier, E.; Jones, M.-C.; Ranger, M.; Leroux, J.-C. *Bull. Tech. Gattefosse* **2003**, *96*, 87−102.
(24) Kim, Y. H. *J. Polym. Sci., Part A: Polym. Chem.* **1998**, *36*, 1685−1698.
(25) Jikei, M.; Kakimoto, M. *Prog. Polym. Sci.* **2001**, *26*, 1233−1285.
(26) Kreutzer, G.; Ternat, C.; Nguyen, T. Q.; Plummer, C. J. G.; Månson, J.-A. E.; Castelletto, V.; Hamley, I. W.; Sun, F.; Sheiko, S. S.; Herrmann, A.; Ouali, L.; Sommer, H.; Fieber, W.; Velazco, M. I.; Klok, H.-A. *Macromolecules* **2006**, *39*, 4507−4516.
(27) Ternat, C.; Kreutzer, G.; Plummer, C. J. G.; Nguyen, T. Q.; Herrmann, A.; Ouali, L.; Sommer, H.; Fieber, W.; Velazco, M. I.; Klok, H.-A. Månson, J.-A. E. *Macromol. Chem. Phys.* **2007**, *208*, 131−145.
(28) Kimmich, R. *NMR−Tomography, Diffusometry, Relaxometry*; Springer: Berlin, 1998.
(29) Stejskal, E. O.; Tanner, J. E. *J. Chem. Phys.* **1965**, *42*, 288−292.
(30) Söderman, O.; Stilbs, P. *Prog. Nucl. Magn. Reson. Spectrosc.* **1994**, *26*, 445−482.
(31) Söderman, O.; Stilbs, P.; Price, W. S. *Conc. Magn. Reson.* **2004**, *23A*, 121−135.
(32) Gostan, T.; Moreau, C.; Juteau, A.; Guichard, E.; Delsuc, M. A. *Magn. Reson. Chem.* **2004**, *42*, 496−499.
(33) Lindblom, G.; Orädd, G. *Prog. Nucl. Magn. Reson. Spectrosc.* **1994**, *26*, 483−515.
(34) Cohen, Y.; Avram, L.; Frish, L. *Angew. Chem., Int. Ed.* **2005**, *44*, 520−554.
(35) Price, W. S. *Annu. Rep. Prog. Chem. Sect. C* **2000**, *96*, 3−53.
(36) Ardelean, I.; Kimmich, R. *Annu. Rep. NMR Spectrosc.* **2003**, *49*, 43−115.
(37) Kärger, J.; Pfeifer, H.; Heink, W. *Adv. Magn. Reson.* **1988**, *12*, 1−89.
(38) Baille, W. E.; Malveau, C.; Zhu, X. X.; Kim, Y. H.; Ford, W. T. *Macromolecules* **2003**, *36*, 839−847.
(39) Rietveld, I. B.; Bedeaux, D. *Macromolecules* **2000**, *33*, 7912−7917.
(40) Ihre, H.; Johansson, M.; Malmstrom, E.; Hult, A. *Adv. Dendritic Macromol.* **1996**, *3*, 1−25.
(41) Leo, A.; Hansch, C.; Elkins, D. *Chem. Rev.* **1971**, *71*, 525−616.
(42) Leo, A. J. *Chem. Rev.* **1993**, *93*, 1281−1306.
(43) Tanner, J. E. *J. Chem. Phys.* **1970**, *52*, 2523−2526.
(44) Callaghan, P. T. *Principles of Nuclear Magnetic Resonance Microscopy*; Clarendon: Oxford, U.K., 1991.
(45) Stejskal, E. O. *J. Chem. Phys.* **1965**, *43*, 3597−3608.
(46) Provencher, S. W. *Comput. Phys. Commun.* **1982**, *27*, 213−227.
(47) Provencher, S. W. *Comput. Phys. Commun.* **1982**, *27*, 229−242.
(48) Morris, K. F.; Johnson, C. S. *J. Am. Chem. Soc.* **1993**, *115*, 4291−4299.
(49) Chen, A.; Wu, D.; Johnson, C. S. *J. Am. Chem. Soc.* **1995**, *117*, 7965−7970.
(50) Cussler, E. L. *Diffusion: Mass Transfer in Fluid Systems*; Cambridge University Press: Cambridge, U.K., 1984.
(51) Cho, C. H.; Urquidi, J.; Singh, S.; Robinson, G. W. *J. Phys. Chem. B* **1999**, *103*, 1991−1994.
(52) Pedersen, J. S. *J. Chem. Phys.* **2001**, *114*, 2839−2846.
(53) Pedersen, J. S.; Gerstenberg, M. C. *Macromolecules* **1996**, *29*, 1363−1365.
(54) Bauer, B. J.; Fetters, L. J.; Graessley, W. W.; Hadjichristidis, N.; Quack, G. F. *Macromolecules* **1989**, *22*, 2337−2347.
(55) Dobashi, T.; Yeh, F.-J.; Ying, Q.; Ichikawa, K.; Chu, B. *Langmuir* **1995**, *11*, 4278−4282.
(56) Schönhoff, M.; Söderman, O. *J. Phys. Chem. B* **1997**, *101*, 8237−8242.
(57) Naylor, A. M.; Goddard, W. A., III. *J. Am. Chem. Soc.* **1989**, *111*, 2339−2341.
(58) Kay, L. E.; Torchia, D. A.; Bax, A. *Biochemistry* **1989**, *28*, 8972−8979.
(59) Parts of this publication are the subject of a patent application: Ouali, L.; Herrmann, A.; Ternat, C.; Plummer, C. J. G.; Klok, H.-A.; Kreutzer, G.; Månson, J.-A. E.; Sommer, H.; Velazco, M. I. PCT Int. Patent Appl., WO 2006/038110, 2006.

MA070222I